Initiation of Apoptosis and Autophagy by Photodynamic Therapy

David Kessel, PhD,[1]* M. Graça H. Vicente, PhD,[2] and John J. Reiners, Jr. PhD[3]
[1]*Departments of Pharmacology and Medicine, Wayne State University School of Medicine, Detroit Michigan 48201*
[2]*Department of Chemistry, Louisiana State University, Baton Rouge Louisiana 70803*
[3]*Institute of Environmental Health Sciences, Wayne State University, Detroit Michigan 48201*

Background and Objectives: This study was designed to examine modes of cell death after photodynamic therapy (PDT).
Study Design: Murine leukemia L1210 cells and human prostate Bax-deficient DU145 cells were examined after PDT-induced photodamage to the endoplasmic reticulum (ER). Phase contrast, fluorescence and electron microscopy were used to identify changes in cellular morphology, chromatin condensation, loss of mitochondrial membrane potential, and formation of phagolysosomes. Western blots were used to assess the processing of LC3-I to LC3-II, a marker for autophagy. Inhibitors of apoptosis and/or autophagy were used to delineate the contributions of the two pathways to the effects of PDT.
Results: Both apoptosis and autophagy occurred in L1210 after ER photodamage with the latter predominating after 24 hours. In DU145 cells, PDT conditions causing comparable cytotoxicity only initiated autophagy. PI3-kinase inhibitors suppressed autophagy in both cell lines as indicated by inhibition of vacuolization and LC3 processing.
Conclusions: Both autophagy and apoptosis were observed in L1210 cells following ER photodamage. In the Bax-deficient DU145 cell line only autophagy was observed. Current information suggests that autophagy can function as either a survival or death pathway. We propose that in the context of PDT, this may also be true. Lasers Surg. Med. 38:482–488, 2006. © 2006 Wiley-Liss, Inc.

Key words: apoptosis; autophagy; necrosis; photodynamic therapy

INTRODUCTION

Photodynamic therapy (PDT) involves the photosensitization of neoplastic cells and tissues with porphyrins or related structures that catalyze, upon irradiation, formation of reactive oxygen species [1]. While effects of PDT on tissues also include vascular shutdown and the evoking of immunologic responses, there is also an element of direct cell kill that can reduce the neoplastic cell population by 2–3 logs [1].

It was initially believed that PDT killed cells via necrosis. In 1991, Oleinick's group provided data indicating that PDT could trigger the induction of apoptosis [2]. Numerous subsequent studies have documented the induction of apoptosis in a variety of cell types, by an array of different sensitizers, and a variety of mechanisms. The cytotoxicity of PDT protocols cannot be totally explained by the induction of apoptosis or necrosis. Cells lacking procaspase-3 [3] or Bax [4] die after PDT, but do not display the characteristics of necrotic or apoptotic cell death.

Autophagy is a process whereby cytosol and organelles become encased in vacuoles termed autophagosomes. Following fusion with lysosomes, the contents of the autophagosomes are digested and recycled [5]. Autophagy was originally characterized as a survival response to nutrient deprivation and other forms of cellular stress. However, studies within the past decade clearly indicate that the induction of autophagy can sometimes lead to cell death [6–12]. Indeed, autophagic death is important during development [13], and appears to mediate the cytotoxicity of some anti-cancer agents [14].

Autophagic cell death has morphological and biochemical features that are distinct from both apoptosis and necrosis [15]. Because autophagy develops in a sequential fashion with defined characteristics, it is considered to be a second type of programmed cell death (sometimes referred to as 'type II cell death'). In this study, we assessed the possibility that PDT may induce autophagy, and that type II death contributes to the cytotoxicity occurring in PDT protocols.

MATERIALS AND METHODS

Chemicals and Biologicals

The photosensitizer 9-capronyloxytetrakis (methoxyethyl) porphycene (CPO) was synthesized as described Ref. [16]. Amino acids and tissue culture media were purchased from Sigma-Aldrich (St. Louis, MO), sterile horse serum from Atlanta Biologicals (Lawrenceville, GA), and fluorescent probes from Molecular Probes (Eugene,

Contract grant sponsor: National Cancer Institute; Contract grant numbers: CA 23378, CA 82341; Contract grant sponsor: National Institute of Environmental Health Sciences; Contract grant numbers: ES009392, ES06639; Contract grant sponsor: NIH; Contract grant number: CHE-304833 from the NSF.
*Correspondence to: David Kessel, Department of Pharmacology, WSU School of Medicine, 540, E. Canfield St., Detroit MI 48201. E-mail: dhkessel@med.wayne.edu.
Accepted 1 March 2006
Published online 13 April 2006 in Wiley InterScience (www.interscience.wiley.com).
DOI 10.1002/lsm.20334

OR). Other reagents were provided by Calbiochem and Sigma-Aldridge (St. Louis).

Cell Propagation

Murine leukemia L1210 cells were grown in sealed flasks using Fisher's Medium (Sigma-Aldrich) containing 10% horse serum and supplemented with 1 mM glutamine, 1 mM mercaptoethanol and gentamicin. Since Fisher's medium is no longer commercially available, an approximation of the formula was prepared by supplementing the α-MEM formulation (GIBCO-BRL, Grand Island, NY) with $MgCl_2$ (45 mg/L), methionine (75 mg/L), phenylalanine (30 mg/L), valine (30 mg/L) and folic acid (9 mg/L). The DU145 cell line was propagated as described in Ref. [17].

Western Blots

Cells were lysed and extracts prepared for Western blot analysis as previously described [18]. Aliquots containing 40 μg of protein were used for these assays. Immunofluorescence signals were detected with Vistra ECF western blot reagent (Amersham Biosciences Corp., Piscataway, NJ) using the Storm imaging system (Molecular Dynamics, Sunnyvale, CA). A rabbit polyclonal antibody raised to microtubule-associated protein LC3 was the gift of Dr. Masahiro Shibata (Osaka University Graduate School of Medicine, Japan).

Viability

Clonogenic assays were used to determine loss of viability after PDT. Serial dilutions of L1210 cell suspensions were plated on soft agar. After 7–9 days growth in a humidified chamber under 5% CO_2, colonies were counted and compared with untreated control values. All such experiments were carried out in triplicate. For DU145, sparsely plated cultures were treated, and the number of colonies that developed were compared with control values.

PDT Protocols

L1210[6] cells (7 mg/ml, 3.5×10 cells/ml) were incubated in Fischer's medium with 25 mM HEPES buffer pH 7.4 replacing $NaHCO_3$, to promote pH maintenance at high cell densities. PDT studies involved incubation for 30 minutes at 37°C with 2 μM CPO. Cells were then resuspended in fresh medium and irradiated at 10°C. The light source was a 600 W quartz-halogen lamp with IR radiation attenuated by a 10 cm layer of water and an 850 nm low-pass filter. Irradiation was carried out at 600–650 nm using appropriate band-pass filters (Oriel, Stratford, CT). The cell suspensions were then incubated for an additional time at 37°C as specified in the text.

DU145 cells were grown on cover slips in 3.5-cm diameter dishes. After a 30 minutes sensitization with 2 μM CPO the medium was replaced, and irradiation was carried out using the light source defined above. Cells were then incubated at 37°C until further procedures were carried out.

Wortmannin, LY294002 or zDEVD-fmk were added to culture medium at the time of sensitization.

Phase-Contrast and Fluorescence Microscopy

All images were acquired using a Nikon Eclipse E600 microscope and a SenSys CCD camera (Photometrics, Tucson, AZ). Images were processed using MetaMorph software (Universal Imaging, Downington, PA). A Uniblitz shutter was used to control exposure of the stage to the excitation source. This shutter was configured to open and close with the camera shutter, thereby minimizing photobleaching of fluorescence.

So as to permit comparisons of image brightness, fluorescence images for each probe were acquired under the same exposure conditions. The gray-scale of the 8-bit images ranged from 0 (black) to 256 (white). Image analysis was carried out using the Integrated Morphometry Analysis program provided by MetaMorph. Fluorescence intensity is expressed as the integrated value of all pixels per cell that exceed the inclusive threshold value set at 45.

Electron Microscopy

For these studies, L1210 cells were fixed with glutaraldehyde and osmium tetraoxide, then dehydrated with ethanol. The cell pellets were embedded in epon resin and cut with an ultramicrotome to 70 nm thick.

Fluorescent Probes and Procedures

Fluorescent probes used were Höchst dye 33342 (3 μM, using a 5 minutes incubation at 37°C) for examination of nuclear morphology, tetramethyrhodamine methyl ester (TMRM, 1 μM for 5 minutes at 37°C) to assess mitochondrial membrane potential, and monodansylcadaverine (MDC, 10 μM, 10 minutes incubation) for imaging enhanced lysosomal activity and lysosome-autophagosome fusion products [19]. After labeling, cells were washed once with fresh growth medium and examined by phase-contrast and fluorescence microscopy. Excitation wavelengths were 360–380 nm (HO342, MDC), and 510–560 nm (TMRM). Interference filters were used to isolate the emission fluorescence of HO342 (400–450 nm), MDC (520–560 nm) and TMRM (550–650 nm).

DEVDase Assays

Activation of DEVDase after irradiation was assessed using the fluorogenic substrate DEVD-R110 as described previously [20]. L1210 cells were incubated at 37°C for 10 minutes after irradiation, prior to being harvested for subsequent analyses.

Statistical Procedures

Statistical significance was evaluated by a paired *t*-test. Differences are assumed to be significant if $P<0.01$.

RESULTS

PDT-Induced Apoptosis and Autophagy: L1210 Cells

Phase-contrast and HO33342 labeling of control cells are shown in Figure 1, panels A and E. Sixty minutes after irradiation of CPO-sensitized cells (LD_{90} conditions), an

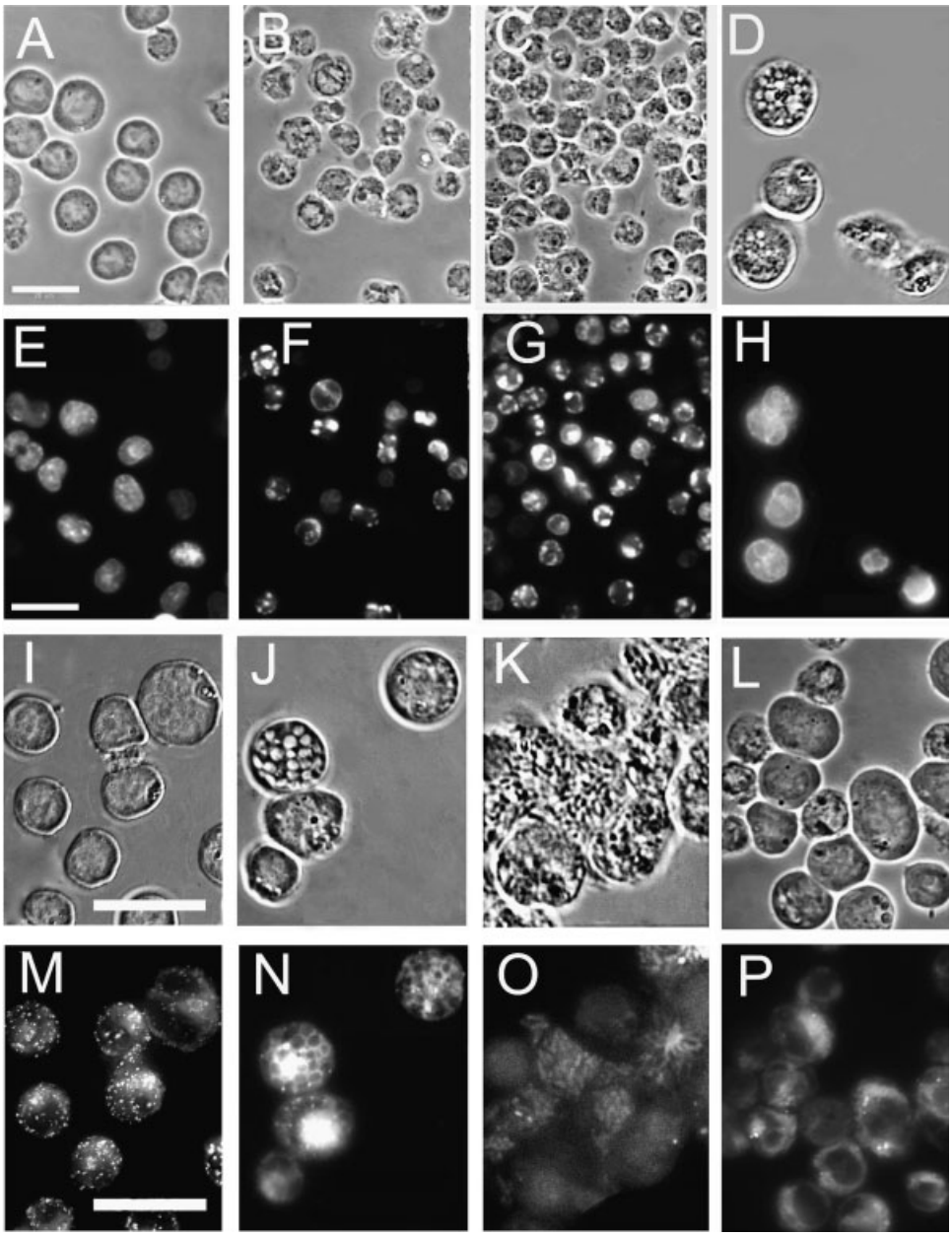

Fig. 1. Effects of an LD_{90} PDT dose (CPO) on morphology and fluorescence labeling of L1210 cells. **A**–**D**, **I**–**L**: phase-contrast images; (**E**–**H**, **M**–**P**) fluorescence. A, E: controls (HO33342 fluorescence); (B, F) 1 hour after irradiation (HO33342 fluorescence); (C, G) 1 hour after irradiation, cultures pre-incubated with 100 nM wortmannin prior to irradiation (HO33342 fluorescence); (D, H) cells 24 hours after irradiation (HO33342 fluorescence); (I, M) controls (MDC labeling); (J, N) cells 24 hours after irradiation (MDC labeling); (K, O) cells 72 hours after irradiation (HO33342 fluorescence). L, P: Cells 72 hours after irradiation with zDEVD and wortmannin present (MDC labeling). White bars apply to each row and represent 10 μ for (A–H) and 20 μ for (I–P).

apoptotic morphology was exhibited in approx. fifty percentage of cells, as detected by HO33342 labeling (Fig. 1F). Some vacuoles can be seen in some cells of the corresponding phase-contrast image of the same field (Fig. 1B). When cells were incubated with wortmannin prior to irradiation a greater percentage of the cells were smaller and displayed apoptotic nuclei (Figs. 1C and G). After 24 hours, the apoptotic cells had disappeared from the population and mainly swollen cells with extensive vacuole formations were observed (Fig. 1D and H).

At a higher magnification, the pattern of MDC labeling in control cells can be observed (Fig. 1M), representing the lysosomal/endosomal population. The pattern was substantially different 24 hours after an LD_{90} PDT dose, with

vacuolated cells (Fig. 1J) showing strong MDC labeling at their periphery (Fig. 1N). In addition to its ability to label normally acidic organelles, MDC has an affinity for fused autophagosomes [19]. At this time, most of the cell population was impermeable to propidium iodide (data not shown). After an additional 48 hours (72 hours post PDT), the predominant cell population exhibited a chaotic morphology (Fig. 1K) that stained weakly with HO33342 (Fig. 1O). Virtually all PDT-treated cells at this time point were permeable to propidium iodide. In contrast, cells exhibited a much more normal morphology 72 hours after PDT when both zDEVD and wortmannin were present (Fig. 1L), although the MDC labeling pattern was indistinct (Fig. 1P). HO33342 labeling revealed no evidence of apoptosis, and the cells were impermeable to propidium iodide (data not shown).

Electron microscopy demonstrated that the vacuoles visualized 24 hours after PDT were not empty (Fig. 2).

PDT-Induced Death of DU145 Cells

The DU145 prostate cell line lacks Bax [17]. This line dies following sensitization with a mitochondrial PDT sensitizer and irradiation, but the mode of death appears to be neither necrotic nor apoptotic [4]. We found that DU145 cells can be killed by PDT protocols employing the endoplasmic reticulum (ER) photosensitizer CPO. However, death was not accompanied by the development of apoptotic morphological features (compare Fig. 3A and B), loss of mitochondrial potential (compare Fig. 3G and H), formation of condensed nuclear chromatin (Fig. 3I), or the activation of pro-caspases 3/7 (data not shown). Instead, CPO sensitized DU145 cultures treated with an LD_{90} PDT dose resulted in the appearance of vacuolated cells (Fig. 3B) that labeled strongly with MDC (Fig. 3E). Co-treatment of CPO-sensitized/irradiated DU145 cultures with the PI3-kinase inhibitor LY294002 effectively suppressed both vacuolization (Fig. 3C) and staining with MDC (Fig. 3F). These latter studies are significant since PI3-kinase activity is required for the development of autophagy [5,6]. These data suggest that CPO-mediated photo killing of the DU145 cell line was associated with the induction of autophagy and not apoptosis.

A further analysis of MDC labeling of control cells and cells 24 hours after an LD_{90} PDT dose was carried out using the MetaMorph Integrated Morphometry Analysis, using 8 bit images (256 step gray-scale). Cells were digitally processed to exclude all pixels with a gray-scale value below 45, that is, the darker pixels. The average gray value was then assessed for each cell. The analysis (Table 1) indicates

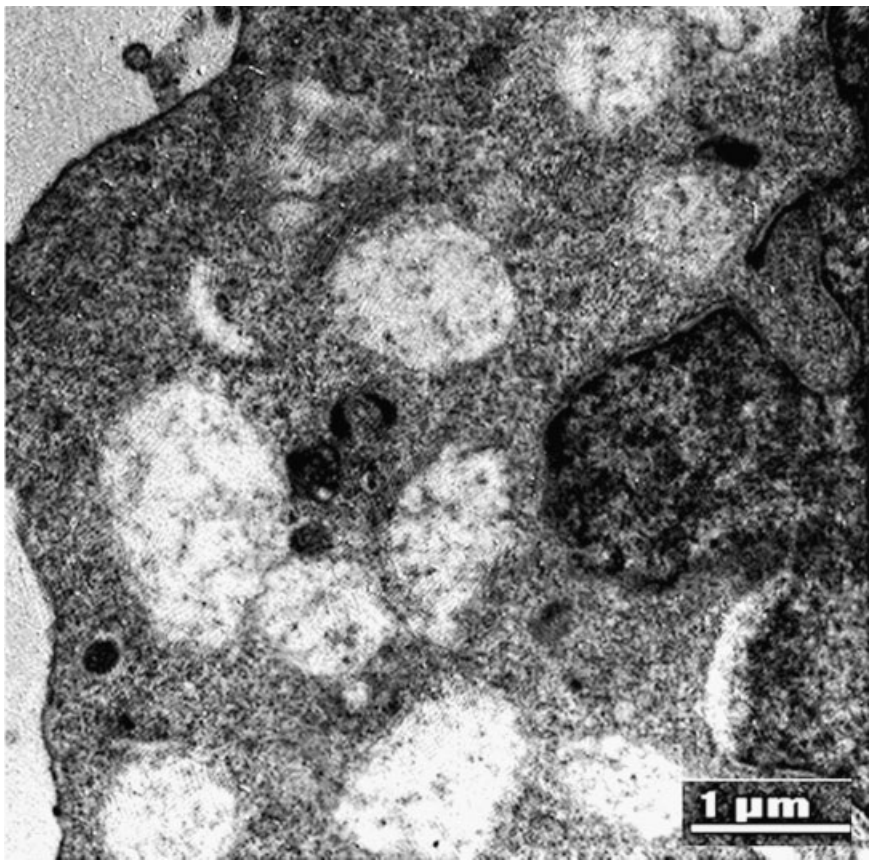

Fig. 2. Electron microscopy showing fine structure of vacuoles in L1210 cells 24 hours after an LD_{90} PDT dose (CPO).

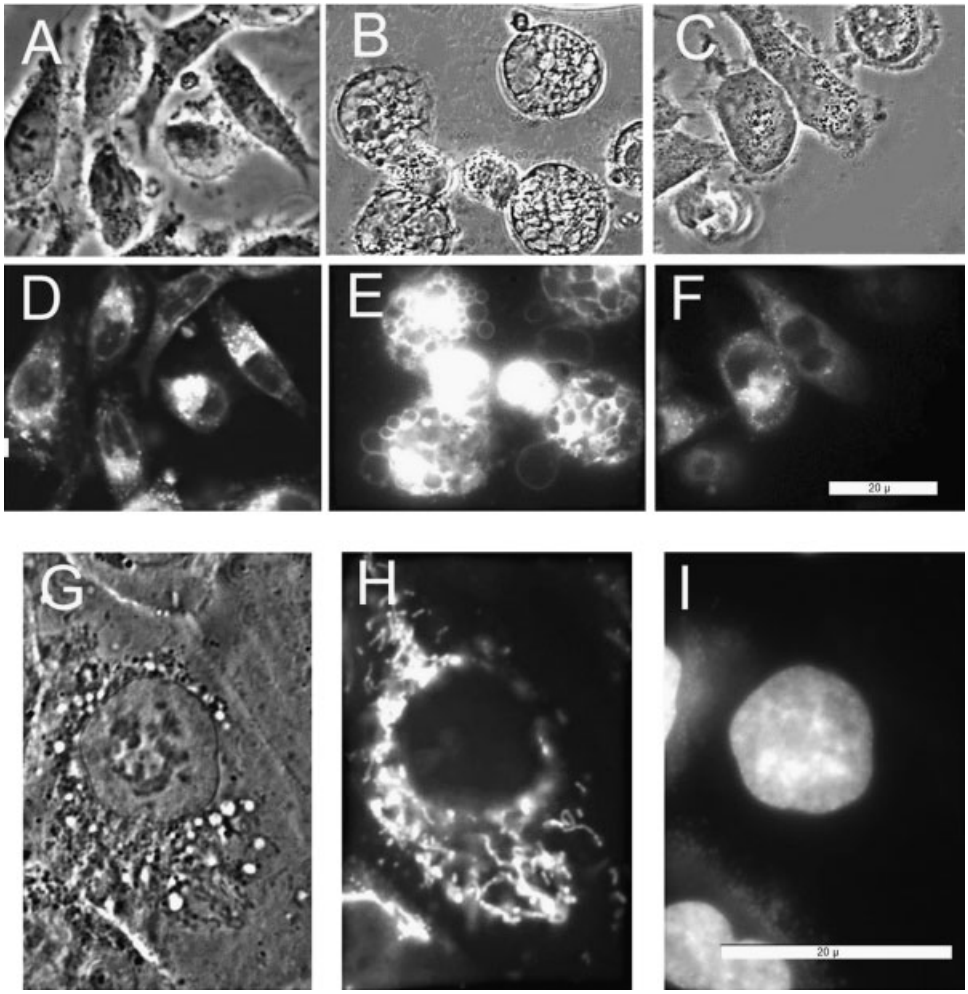

Fig. 3. Phase-contrast (**A**–**C**, **G**) and fluorescence (**D**–**F**, **H**, **I**) images of DU145 cells. A, D: control cells (phase-contrast vs. MDC labeling); (B, E) cells 24 hours after an LD_{90} PDT dose using CPO (phase-contrast vs. MDC); (C, F) phase contrast versus MDC labeling 24 hours after PDT with LY294002 (25 μM) present. Images (G–I) are of a single cell 24 hours after PDT: (G) phase-contrast, (H) TMRM labeling showing maintenance of the mitochondrial membrane potential, (I) HO33342 labeling showing absence of apoptotic morphology. White bars = 20 μ.

that there was approximately a fourfold increase in the number of bright pixels after PDT compared with untreated controls and that this difference was abolished in the presence of 100 nM wortmannin.

TABLE 1. Integrated Morphometry Analysis of MDC Labeling of DU145 Cells

Treatment	Relative Intensity	n
None	100 ± 12	25
PDT	351 ± 44*	29
PDT + wortmannin	95 ± 18	23

Effects of an LD_{90} PDT dose with CPO on pixel brightness of MDC fluorescence in DU145 cells. Data represent the mean ± SD for the specified number of cells.
*Statistical significance ($P < 0.01$) compared with controls.

LC3 Processing

Upon the induction of autophagy, the cytosolic protein LC3-I is covalently linked to phosphatidylethanolamine to yield LC3-II, which subsequently associates with the autophagosome [21]. Conversion of LC3-I to LC3-II has been used as a marker for autophagy [20]. Irradiation of L1210 or DU145 cultures that had been presensitized with CPO resulted in a conversion of LC3-I to LC3-II. LC3 processing was markedly decreased when either cell line was preincubated with wortmannin (100 nM) prior to irradiation. In contrast, incubation with 50 μM zDEVD-fmk prior to PDT potentiated LC3-I processing (Fig. 4).

Effects of Apoptosis and Autophagy Inhibitors

A study of the effects of inhibitors of apoptosis versus autophagy on DEVDase activation provided additional

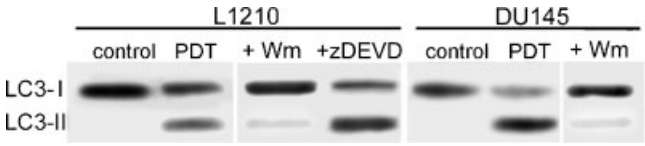

Fig. 4. Western blot analyses of LC3-I processing. From the left: control L1210 cells; cells 24 hours after an LD_{90} PDT dose with CPO; 24 hours after PDT with 100 nM wortmannin present during sensitization with CPO; 24 hours after PDT with 50 μM zDEVD-fmk present during the sensitization with CPO; control DU145 cells; DU145 cells 24 hours after an LD_{90} PDT dose with CPO; and 24 hours after PDT with 100 nM wortmannin present during the sensitization with CPO. Each lane contained 40 μg of protein.

information on the relationship between the two processes (Table 2). In these studies L1210 cultures were exposed to CPO/PDT conditions yielding a 90% loss of viability. DEVDase activity was clearly increased consistent with the initiation of apoptosis, and this activation was abolished when the caspase 3/7 inhibitor zDEVD-fmk was present. In agreement with the chromatin condensation studies depicted in Figure 1F and G, DEVDase activation was elevated when autophagy was impaired by the presence of wortmannin, but reduced to the control value when both inhibitors were present.

DISCUSSION

In the current study we used multiple criteria to score for the development of autophagy. Amongst our criteria were: (1) The development of multiple large vacuoles whose periphery was labeled with MDC; (2) suppression of vacuole formation and MDC labeling by inclusion of a PI3-kinase inhibitor; (3) demonstration of the vacuoles not being empty by electron microscopy; (4) conversion of LC3-I to LC3-II; (5) maintenance of mitochondrial membrane potential; and (6) the absence of nuclear condensation. A comparison of panels 1A and 1D, and of 1I and 1J indicate that the vacuolated cells are larger than their non-treated counterparts. We conclude that PDT-induced ER photodamage induces autophagy in both L1210 and DU145 cultures. To the best of our knowledge, these are the first studies to document PDT-induced autophagy.

TABLE 2. Effects of zDEVD-fmk and Wortmannin on DEVDase Activation after PDT

Treatments	DEVDase activity
None	0.39 ± 0.03
PDT	8.5 ± 0.53
PDT + zDEVD-fmk	0.66 ± 0.21*
PDT + wortmannin	10.3 ± 0.71*
PDT + both	0.48 ± 0.23*

Effects of an LD_{90} PDT dose with CPO on DEVDase activity of L1210 cells. Where specified, wortmannin (100 nM) and/or zDEVD-fmk (50 μM) were present at the time of loading with sensitizer. DEVDase activity is expressed in terms of nmol product/min/mg protein. Data represent the mean ± SD for three determinations.

*Statistical significance ($P < 0.01$) compared with PDT-treated cells without additions.

The data presented in Figure 1 indicate that both apoptosis and autophagy occur in L1210 cultures following PDT with CPO. The appearance of apoptotic cells, as well as their disappearance from the cultures, occurred quickly after PDT with CPO. Apoptotic cells were obvious within an hour of PDT, and disappeared from the cultures within the subsequent 23 hours. In contrast, the appearance of cells with autophagic characteristics required ~24 hours. The relative percentages of L1210 cells undergoing apoptosis or autophagy following PDT could be experimentally manipulated. Preincubation with the PI3-kinase inhibitors wortmannin or LY294002 prior to PDT promoted the morphological appearance of apoptosis (compare Fig. 1F with G) and DEVDase activation (Table 2), and suppressed vacuole formation, MDC labeling, and the conversion of LC3-I to LC3-II in L1210 cultures. These effects probably reflect inhibitions of both the class III PI3 kinases needed for autophagy, and the class I enzymes that activate the anti-apoptotic Akt/PKB pathway [12]. Conversely, pretreatment with the caspase-3/7 inhibitor zDEVD-fmk enhanced the conversion of LC3-1 to LC3-II (Fig. 4), and the percentage of L1210 cells developing vacuoles (data not presented). We propose that after PDT there is an equilibrium established between autophagy and apoptosis, with inhibition of either process leading to enhanced activity by the other. This inhibition could be mediated either pharmacologically, or as in the case of DU145 cells, reflect a defect in one of the two pathways that results in a default activation of the other.

Although autophagy was originally described as a cell survival response, numerous studies have also implicated it as a death pathway [6–12]. In the case of PDT with CPO it appears that the induction of autophagy also leads to cell death. The basis for this death, in the context of PDT, possibly lies in the ability of CPO [20], as well as another sensitizer [22] to photodamage Bcl-2. Specifically, the down regulation of Bcl-2 expression by molecular approaches has been shown to induce/facilitate the development of autophagy [23,24].

Oleinick's group had reported that photo killing was not affected in cell lines lacking pro-caspase-3 [3], and proposed that apoptosis may merely be a means for disposing of dead cells. A similar role may hold for autophagy. As in apoptosis, there is a flipping of phosphatidylserine to the cell surface during autophagy [25]. Externalization of this lipid enables the dying cell to be recognized and phagocytized, thus avoiding an inflammatory response.

In the context of PDT, it is interesting to note that autophagy can result in class II presentation of antigens derived from cytosolic proteins [26]. The autophagic response to PDT may therefore provide an explanation for the finding that treatment of tumor cells with low-dose PDT can yield anti-tumor vaccines [27].

REFERENCES

1. Dougherty TJ, Gomer CJ, Henderson BW, Jori G, Kessel D, Korbelik M, Moan J, Peng Q. Photodynamic therapy. J Natl Cancer Inst 1998;90:889–905.
2. Agarwal ML, Clay ME, Harvey EJ, Evans HH, Antunez AR, Oleinick NL. Photodynamic therapy induces rapid cell death by apoptosis in L5178Y mouse lymphoma cells. Cancer Res 1991;51:5993–5996.
3. Whitacre CM, Satoh TH, Xue L, Gordon NH, Oleinick NL. Photodynamic therapy of human breast cancer xenografts lacking caspase-3. Cancer Lett 2002;179:43–49.
4. Chiu SM, Xue LY, Usuda J, Azizuddin K, Oleinick NL. Bax is essential for mitochondrion-mediated apoptosis but not for cell death caused by photodynamic therapy. Br J Cancer 2003;89:1590–1597.
5. Yorimitsu T, Klionsky DJ. Autophagy: Molecular machinery for self-eating. Cell Death Differ 2005;12(Suppl 2):1542–1552.
6. Gozuacik D, Kimchi A. Autophagy as a cell death and tumor suppressor mechanism. Oncogene 2004;23:2891–2906.
7. Yu L, Alva A, Su H, Dutt P, Freundt E, Welsh S, Baehrecke EH, Lenardo MJ. Regulation of an ATG7- beclin 1 program of autophagic cell death by caspase-8. Science 2004;304:1500–1502.
8. Edinger AL, Thompson CB. Death by design: Apoptosis, necrosis and autophagy. Curr Opin Cell Biol 2004;16:663–669.
9. Eskelinen EL. Doctor Jekyll and Mister Hyde: Autophagy can promote both cell survival and cell death. Cell Death Differ 2005;12(Suppl 2):1468–1472.
10. Tsujimoto Y, Shimizu S. Another way to die: Autophagic programmed cell death. Cell Death Differ 2005;12 (Suppl 2): 1528–1534.
11. Lockshin RA, Zakeri Z. Apoptosis, autophagy, and more. Int J Biochem Cell Biol 2004;36:2405–2419.
12. Guillon-Munos A, van Bemmelen MX, Clarke PG. Role of phosphoinositide 3-kinase in the autophagic death of serum-deprived PC12 cells. Apoptosis 2005;10:1031–1041.
13. Yue Z, Jin S, Yang C, Levine AJ, Heintz N. Beclin 1, an autophagy gene essential for early embryonic development, is a haploinsufficient tumor suppressor. Proc Natl Acad Sci USA 2003;100:15077–15082.
14. Kondo Y, Kanzawa T, Sawaya R, Kondo S. The role of autophagy in cancer development and response to therapy. Nat Rev Cancer 2005;9:726–734.
15. Kroemer G, El-Deiry WS, Golstein P, Peter ME, Vaux D, Vandenabeele P, Zhivotovsky B, Blagosklonny MV, Malorni W, Knight RA, Piacentini M, Nagata S, Melino G. Classification of cell death: Recommendations of the nomenclature committee on cell death. Cell Death Differ 2005;12 (Suppl 2): 1463–1467.
16. Toledano H, Edrai R, Kimel S. Photodynamic damage by liposome-bound porphycenes: Comparison between in vitro and in vivo models. J Photochem Photobiol B Biol 1998;42: 20–27.
17. Tang DG, Li L, Chopra DP, Porter AT. Extended survivability of prostate cancer cells in the absence of trophic factors: Increased proliferation, evasion of apoptosis, and the role of apoptosis proteins. Cancer Res 1998;58:3466–3479.
18. Kim HR, Kessel D. Enhanced apoptotic response to photodynamic therapy after bcl-2 transfection. Cancer Res 1999; 59:3429–3432.
19. Biederbick A, Kern HF, Elsasser HP. Monodansylcadaverine (MDC) is a specific in vivo marker for autophagic vacuoles. Eur J Cell Biol 1995;66:3–14.
20. Kessel D, Castelli M, Reiners JJ Jr. Apoptotic response to photodynamic therapy versus the Bcl-2 antagonist HA14-1. Photochem Photobiol 2002;76:314–319.
21. Bampton ETW, Goemans CG, Niranjan D, Mizushima N, Tolkovsky AM. The dynamics of autophagy visualised in live cells: From autophagosome formation to fusion with endo/lysosomes. Autophagy 2005;1:23–36.
22. Xue LY, Ohiu SM, Oleinick NL. Photochemical destruction of the Bcl-2 oncoprotein during photodynamic therapy with the phthalocyanine photosensitizer pc4. Oncogene 2002;76:314–319.
23. Saeki K, Yuo A, Okuma E, Yazaki Y, Susin SA, Kroemer G, Takaku F. Bcl-2 down-regulation causes autophagy in a caspase-independent manner in human leukemic HL60 cells. Cell Death Differ 2000;7:1263–1269.
24. Pattingre S, Tassa A, Qu X, Garuti R, Liang XH, Mizushima N, Packer M, Schneider MD, Levine B. Bcl-2 antiapoptotic proteins inhibit Beclin 1-dependent autophagy. Cell 2005; 122:927–939.
25. Melino G, Knight RA, Nicotera P. How many ways to die? How many different models of cell death? Cell Death Differ 2005;12 (Suppl 2):1457–1462.
26. van der Bruggen P, Van den Eynde BJ. Processing and presentation of tumor antigens and vaccination strategies. Curr Opin Immunol 2006;18:98–104.
27. Gollnick SO, Vaughan L, Henderson BW. Generation of effective antitumor vaccines using photodynamic therapy. Cancer Res 2002;62:1604–1608.